International Journal of Applied Engineering Research ISSN 0973-4562 Volume 16, Number 8 (2021) pp. 696-708

A System Dynamics Model for the Study of Fixed Bed Grain Dryers

Alex Rodrigo Magalhães Pessoa[1] and Rafael Pinheiro Amantéa[2,*]

[1]*IETEC – Instituto de Educação Tecnológica (Departamento de Engenharia e Gestão de Processos e Sistemas) Address: Rua Tomé de Souza, 1065, Postal Address: 30180-111, Brazil.*

[2]*Institution: IETEC – Instituto de Educação Tecnológica (Departamento de Engenharia e Gestão de Processos e Sistemas) Address: Rua Tomé de Souza, 1065, Postal Address: 30180-111, Brazil.*

Abstract

Reducing grain moisture content by drying is a typical agriculture and food engineering strategy to increase storage and commercialization. However, drying is an industrial process with high energy consumption and demands efficient equipment design. In most cases, the inherent transport phenomena are modeled by partial differential equations that demand numerical techniques and advanced computer programming skills. System dynamics is a powerful tool for modeling and solving complex systems and is used in many knowledge areas. The modeling and solution of complex system dynamics models are done by friendly interface and low complexity software. According to the system dynamics perspective, this paper presents a fixed bed dryer's modeling based on classic partial differential equations of energy and continuity. Calibration tests were realized using the pure convection equations as a reference. Spatial profiles of the main variables were presented and validated according to reference data obtained by another numerical method. Different scenarios were generated, varying the input quantities. With a mean error related to the reference literature below 10%, the obtained results allow us to conclude that the proposed methodology can be used as a solution tool of systems involving partial differential equations. Specifically, to the design, research, and evaluation of the operational grain dryers' conditions, the proposed model opens the field to the construction and study of spatial system dynamics models, thus enabling the analysis of population dynamics of plagues, evaluation of the product quality during drying, aeration and cooling operations, as well as another complex interaction between macro and microsystems related to drying, and also the investigation of the process optimization.

Keywords: System dynamics. Drying. Simulation.

1 INTRODUCTION

Considering the perishable characteristic of grains and food, drying stands out against the other conservation methods, considering the cost-benefit ratio and the extension of the product storage time [1]. In the chemistry and food processing industries drying or dehydration represent a preponderant stage. Using this, the deterioration due to chemical and microbiological reactions is widely minimized to reduce the product humidity level.

Industrial drying processes are recognized as important consumers of fossil source energy[2].

Therefore, it is necessary to develop new efficient food drying techniques. Industrial dryers research focuses on basing the enhancement of these equipment projects and enabling producers to know or estimate the characteristics of grains during and after the process. In this context, there are innumerable approaches and methodologies of quantitative analysis. In general, the literature on the design and simulation of grain drying classifies the mathematical models as thin or deep layer models.

The thin layer study describes heat and water mass transfer between the environment air and the grain surface or describes the water diffusion inside the grain [3]. In the deep layer drying modeling, the mass (moisture) transport phenomena between the grains are considered beyond the characteristics above. These are mostly convective.

Many of the physical problems are mathematically described using partial differential equations that represent the relations between various rates of the involved quantities. These models may present formulations with convection, diffusion, and convection-diffusion therms that belong to a specific set of propagation problems [4].

In most cases, the analytical solution of these equations is impractical, mainly in situations of two and three spatial dimensions. Additionally, the presence of convective therms and nontrivial boundary conditions may be impeditive to develop analytic solutions [5]. Thereby, numerical approximations as solution strategies become necessary. Specific to the study of drying problems, different methodologies of this type have been used, like the finite differences method [6], finite elements [7], finite volumes [8], and radial basis functions [3]. Applying these numerical methodologies to the solution of partial differential equations involves the knowledge and ability in programming languages

* Corresponding author

and mathematical modeling dealing with transport phenomena inherent in the process.

On the consulted literature, the finite differences method showed up to be the most used to solve the deep layer food drying models [9][10][11] [12] [6]) and in several cases, experiments validated the results.

On the study of soy, [13] compared numerical methods simulations with experimental data. For the drying process, techniques of finite difference and finite volume were used. For aeration, the finite element method was used.

[14] implemented the techniques of finite element and finite volume and obtained results very close to those from a reference work, which used the finite difference method.

[3] took advantage of the radial basis function technique to solubilize the drying equations.

The system dynamics technique is being applied to troubleshooting and modeling of problems of a wide range of knowledge areas, such as social studies, management, environment, and mechanics, among others [15].

On business, [16] presents multiple examples and subject-specific approaches to the technique and modeling, such as delay types, decision processes, floating goals, nonlinearities, resource constraints, and initial conditions. [17] analyze the competitiveness of business clusters. [18] suggest policies and guidelines referred to enterprise logistic processes outsourcing.

In the management field, we can quote the work of [19], who propose an alternative model to the traditional techniques of construction project control. [20] developed models to base the decision-making in the artisanal dredge fisheries administration. Operational and strategic management is common in multidisciplinary literature related to evaluating the financial and environmental impact [e.g., [21] addressing the reuse of electronic waste]. [22] present a system dynamics model of the interrelationships of the subjects involved in the concept of one health, present in the medical area. [23] explore the economic, environmental, and social aspects and the sustainability of agricultural production.

[24] used the methodology to calculation several variables and parameters related to water quality in rivers, both in steady-state and transient, corroborating with the proposal of the present work of solving differential equations by system dynamics, discretizing the problem physically using the finite difference numerical method and using Taylor series approximation.

As an alternative to the traditional numerical techniques to analyze these sets of partial differential equations, system dynamics is a possible strategy to model and solve complex systems. This method simulates the behavior of systems over time, based on the causal relations between their internal and external elements, as well as the effects of feedback and delay among them. The objective is to understand the system's operation on a macro level, using a model built according to the interactions of all involved [23].

Besides allowing the study of the relations of the variables that make up the system, system dynamics draws attention because of the low complexity math inherent in the technique and simple implementation of algorithms using a language substantiated on diagrams. Thereby, simulations of problems whose modeling is of high complexity can be easily done in software such as Vensim, Stella/Ithink, and Anylogic.

In this context, the main purpose of the present work is to perform the modeling and simulation of the fixed bed grain drying process using the system dynamics methodology.

In a specific manner, it is aimed:

- To implement and perform calibration tests to solubilize convection-type differential equations by employing Anylogic software;
- To develop the causal and flux diagram to the fixed layer drying model proposed by [25]
- To validate the results obtained using data available in the literature;

In the search process realized during the literature review of this text, similar scientific productions were not found, that is, which used system dynamics to compute the variables of deep layer fixed bed grain drying, which highlights the innovative character of the work.

2 MATERIALS AND METHODS

2.1 The one-dimensional mathematical model for the deep layer drying process

This work uses a one-dimensional mathematical model based on the mass and energy conservation equations and thin layer drying equation [26].

Taking the dryer as the control volume, the continuity equation for the air moisture is: the moisture variation rate generated inside the control volume is equal to the mass variation rate inside it plus the mass net flux through the control surface. In this case, are not considered the moisture accumulation terms. Thereby the expression becomes:

$$\frac{\partial W}{\partial t} = -\frac{V}{\varepsilon}\frac{\partial W}{\partial x} - \frac{\rho_p}{\varepsilon \rho_a}\frac{\partial M}{\partial t} \quad (1)$$

The air energy balance inside the dryer is based on the first law of thermodynamics. Thus, the heat transferred to the grain mass equals the enthalpy variation rate inside the control volume, summed up to the enthalpy net flux through the control surface. Neglecting the enthalpy accumulation, we have:

$$\rho_a \varepsilon \frac{\partial T}{\partial t} = -V \rho_a \frac{\partial T}{\partial x} - \frac{h' a (T-\theta)}{(c_a + W c_v)} \quad (2)$$

The energy balance applied to the grains establishes that the energy transferred from the air to the grains by convection corresponds to the sum of the enthalpies needed to warm up the grains and evaporate the water inside the grain (product).

$$\frac{\partial \theta}{\partial t} = \frac{h' a (T-\theta)}{\rho_p c_p} + \frac{[h_{fg} + c_v (T-\theta)]}{c_p}\frac{\partial M}{\partial t} \quad (3)$$

The system made by equations (1), (2), and (3) has four dependent variables: W, T, θ and M. The additional equation that enables the resolution is the local drying rate or thin layer

drying rate. In the present work, the thin layer grain drying process is approximated by the one-grain drying model. The thin layer drying equation proposed by Thompson, Peart, and Foster (1968) was adopted, presented below.

$$\frac{\partial M}{\partial t} = \frac{M_e - M}{3600\sqrt{A^2 + \frac{Bt}{900}}} \quad (4)$$

In the simulation of the corn model, Factors A and B depend on the product and the conditions of the drying process.

The calculation of the equilibrium moisture content was executed by the equation:

$$M_e = \sqrt{\frac{\ln(1-RH)}{-0{,}688(T-46)}} \quad (5)$$

2.2 System dynamics

System dynamics is a technique that aims to facilitate the comprehension of the behavior of complex systems in function of time [20][21]. It is a graphic method based on systems thinking that enables qualitative and quantitative systems analysis [19].

On the qualitative modeling, diagrams of the causal relations are built. These are also known as causal loops diagrams or simply causal diagrams. Using quantitative modeling, the flux diagrams are elaborated [23]

On the causal diagram, the relations between the variables are represented by arrows. According to the type of influence that an item provokes on another, these are accompanied by the positive (+) or negative (-) signal. If an increase in the value of a variable causes an increase in the value of another and a decrease in the value of the first causes a decrease in the value of the second, we have a positive relation. Otherwise, we have a negative relation

The occurrence of feedback or loop paths between the variables is common. When the number of negative relations in the variables of a loop is odd, this is negative, also known as a balancing loop. In the same way, a positive or reinforcement loop has an even number of negative relations [15]. This characterization directly implies the stability of a system because positive loops provoke exponential growths, with consequent instability. Negative loops provoke a decrease in the values of the variables, providing stability.

The variables can be common in the flux diagrams, from stock-type or flux-type, and their equations must be attributed. The stored volume can be considered a stock whose value will always depend on the input and output fluxes and the initial volume, as is showed in Figure 1.

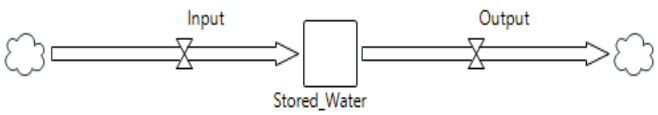

Figure 1. Flux diagram of a water tank.

Generally, the software for simulating system dynamics uses flux diagrams. In addition to drawing the diagram, the user must provide the values or equations to define each variable, the stock's input and output fluxes, and their initial values. Also, the simulation time unit, time step and final time must be configured.

Additionally, it is common for the simulators to allow the configuration of other data, such as the resolutions numerical methods and the creation of graphics and tables with the values of the variables.

In the simulations presented in this work, the Anylogic program was used, and the results were exported to sheets in Excel format, where the graphics were plotted.

2.3 Causal diagram of the deep layer drying process

In the system dynamics' perspective, the deep layer grain drying process described in equations (1) to (4) can be synthesized by the causal diagram in Figure 2:

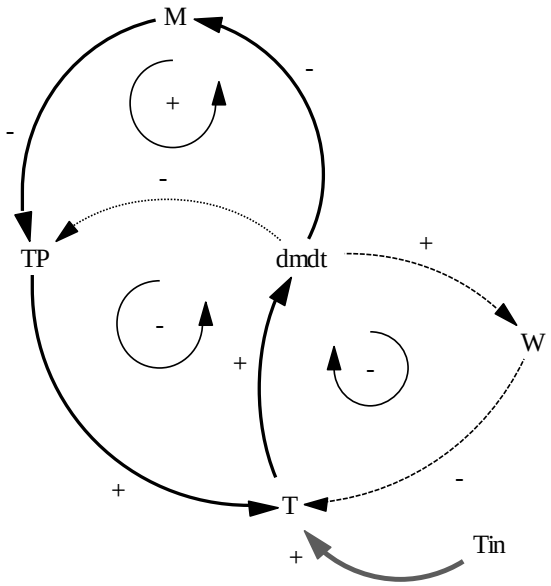

Figure 2. Causal diagram of deep layer drying.

As can be observed, there are three loops on the diagram, being one of reinforcement and two of balance. The reinforcement loop is responsible for the maintenance of the drying process inside the dryer, as follows.

An increase in air temperature (T), obtained in the function of the inlet air temperature (Tin), for example, causes the growth of the drying rate (dmdt). How higher is the drying rate, lower is the product water content (M). The reduction of the product water content causes the rise of the grain temperature (TP). Grain and air temperature tend to be always in equilibrium. Thus, this also increases the air temperature inside the dryer, restarting the loop process. The arrows identify this path with continuous lines and positive signs on the diagram.

The balance loops, identified by the dashed lines and negative signs stabilize the system, attenuating the effect of the positive loop.

The causal relations of the most left-positioned negative loop demonstrate that an increase in the air temperature inside the dryer (T) causes the elevation of the drying rate (dmdt). The higher this rate (that is, in the function of the amount of water removed from the grain), the more difficult it is to warm it (TP). On the loop closing, with the decrease of the grain temperature, we have the reduction of the air temperature inside the dryer.

The negative loop at the rightest position shows that an increase of the drying rate (dmdt), due to the elevation of the air temperature inside the dryer (T), causes the growth of the amount of water in the air (W). The higher this humidity level, the lower the air temperature inside the dryer, restarting the loop process.

2.4 Spatial discretization of partial differential equations using fluxes, stocks, and variables

As exposed in [4], the one-dimensional pure convection equation to any function f (y,t) has the form:

$$\frac{\partial f}{\partial t} + u\frac{\partial f}{\partial y} = 0 \tag{6}$$

Considering the specific case of a tube being flowed by an incompressible fluid (liquid), the temperature distribution along the same can be determined by:

$$\frac{\partial T}{\partial t} + u\frac{\partial T}{\partial y} = 0 \tag{7}$$

In this thermal convection problem, the initial tube temperature distribution must be previously known.

Rearranging the terms of the previous equation, we have:

$$\frac{\partial T}{\partial t} = -u\frac{\partial T}{\partial y} \tag{8}$$

The Taylor series second-order finite differences approximation to this expression is [4]

$$\frac{\partial T}{\partial t} = -u\frac{3T(y,t)-4T(y-dy,t)+T(y-2dy,t)}{2dy} \tag{9}$$

Dividing the tube into a finite length consecutive segments set, we have a model of what happens at each one of them individually. By connecting them in a cascade, we can then reproduce the behavior of the whole tube. This methodology is analogous to the thermal diffusion equation discretization presented previously.

The flux diagram of this problem is represented in Figure 3.

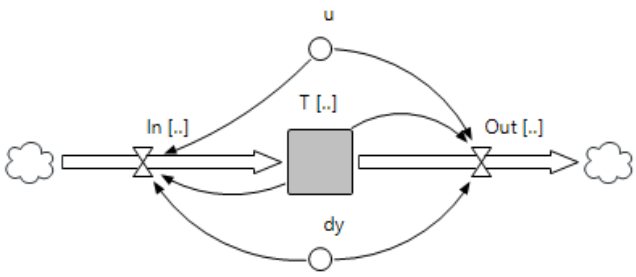

Figure 3. Pure convection equation representation in the Anylogic software.

Given the negative sign before u in the equation (8) and, as already cited, because the software considers in the stock variables calculation the entering fluxes minus the out fluxes, to the implementation of this modeling, we must assume the below equations, to a discretization with n+1 point:

$$\begin{cases} In[i] = 2 \cdot u \cdot \frac{T[i-1}{dy} \\ Out = u \cdot \frac{3 \cdot T[i]+T[i-2]}{2 \cdot dy} \\ i = 2,3,4,\dots,n \end{cases} \tag{10}$$

In short, by the flux diagram is perceived that the calculation of the variation in the temperature stock (positive and negative fluxes) in each one of the points to a thermal convection situation depends on the constant u, the temperature on the point itself and the near points and the discretization, level assumed to the problem resolution (dy).

Once the approximate computation above uses two preceding points and the point i=1 has only one preceding, first-order approximation must be assumed, whose fluxes are calculated by

$$\begin{cases} In[1] = u \cdot \frac{T[0]}{dy} \\ Out[1] = u \cdot \frac{T[1]}{dy} \end{cases} \tag{11}$$

It was considered null variation for the point i=0 (boundary condition).

2.4.1 Discretization of the one-dimensional mathematical model of the deep layer drying process

From the analysis of the four equations already presented that compound the one-dimensional mathematical model of the deep layer drying process, it is possible to observe that they are based on four principal variables: M, W, T and θ.

Considering that it is fundamental to know the magnitude of these variables in the function of time during the simulation and that the mentioned equations offer expressions for the time-varying ratio of each of these physical quantities, they must constitute the stocks of the flow diagram on the system dynamics modeling.

Due to the number of involved variables, to build the complete diagram of the deep layer drying process, the first step is to obtain the simplified diagrams of M, W, T, and θ, which are built using relations of these same stocks, the flows that go in and out of them (positive and negative variation ratio) and others related quantities.

Consider initially the first law of thermodynamics applied to the drying air [equation (2)]. Isolating the derivative of the temperature concerning the time on the left side of the equation, we have:

$$\frac{\partial T}{\partial t} = -\frac{V}{\varepsilon}\frac{\partial T}{\partial x} - \frac{1}{\varepsilon\rho_a}\frac{h'a(T-\theta)}{(c_a+Wc_v)} \tag{12}$$

Using the same discretization process of equations (1), (2), and (3), based on the approximation of derivatives by the Taylor series, it is possible to divide the first term on the right into two parcels. One that contributes to the temperature increase

(entering flux) and one that contributes to the decrease (outflux). The source term expression contributes to elevating the air temperature and must be considered on the entering flux.

The simplified flux diagram representing equation (2) becomes Figure 4, where the variable TP is the product temperature theta. At this point, it is not the focus to detail the calculation of the fluxes that enter and exit of W and theta, but rather demonstrate that these stocks influence the T fluxes.

In Table 1, we have the expression to calculate entering and exiting fluxes of the stock T (air temperature) of Figure 4.

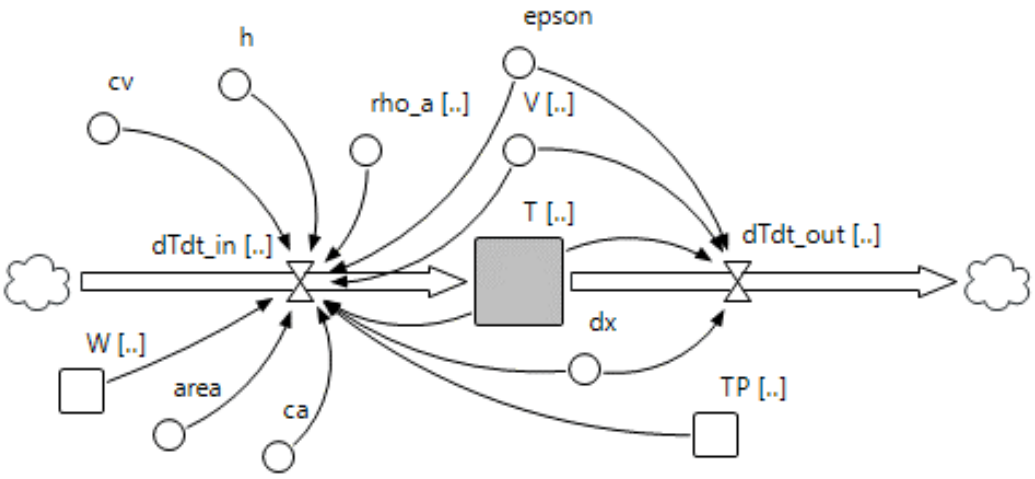

Figure 4. Air temperature simplified flux diagram.

Table 1. Expressions for the fluxes of the stock T.

Layer $[i]$	**Input flux (dTdt_in)**	**Output flux (dTdt_out)**
0	0 (boundary condition)	0 (boundary condition)
1	$T[0]\frac{V}{dx\cdot\varepsilon}-\frac{1}{\varepsilon\rho_a}\frac{h'a(T[1]-\theta[1])}{(c_a+W[1]c_v)}$	$T[1]\frac{V[1]}{dx\cdot\varepsilon}$
From 2 to n	$4\cdot T[i-1]\frac{V}{2\cdot dx\cdot\varepsilon}-\frac{1}{\varepsilon\rho_a}\frac{h'a(T[i]-\theta[i])}{(c_a+W[i]c_v)}$	$(3\cdot T[1]+T[i-2])\frac{V[1]}{2\cdot dx\cdot\varepsilon}$

In sequence, the procedure is detailed to obtain the simplified flux diagram for the product moisture content stock – M.

As established by the thin layer drying equation [equation (4)], the variation of the product moisture content in the function of time depends on the current content, the equilibrium moisture content, air temperature, and time. Because the physics of the problem does not allow the humidity to increase, the expression is related to the flux exiting the stock.

Therefore, this simplified flux diagram corresponds to Figure 5, where the variable named factor calculates the expression that contains the variables A and B of equation (4). In this context, the flux expression that enters the stock is null (dMdt_in [i]=0).

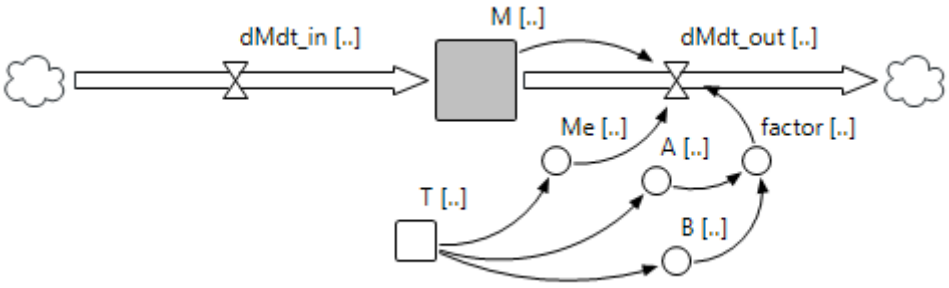

Figure 5. Product moisture content simplified flux diagram.

The expression related to the flux that exits the stock M – product moisture content on the diagram of Figure 5 is:

$$dmdt_{out[i]} = -(M_e[i] - M[i]) \cdot fator[i] \quad (13)$$

Similarly, as defined by the equation of steam continuity on the air [equation (1)], there is moisture accumulation (left side of the expression) if there is a positive balance (the term on the right side that has the derivative of moisture in relation of space) or if there is loss of water from the grain to the air (the term on the right side that has the derivative of the product moisture content in relation of time).

Based on this physical comprehension of the expression, it is possible to model the simplified flux diagram of the air humidity ratio (W), according to Figure 6.

The expressions to calculate the fluxes that go in and out of the stock W on the flux diagram of Figure 6 depend on the index (layer) and are described in the next table. These were obtained by the same procedure of discretization already used.

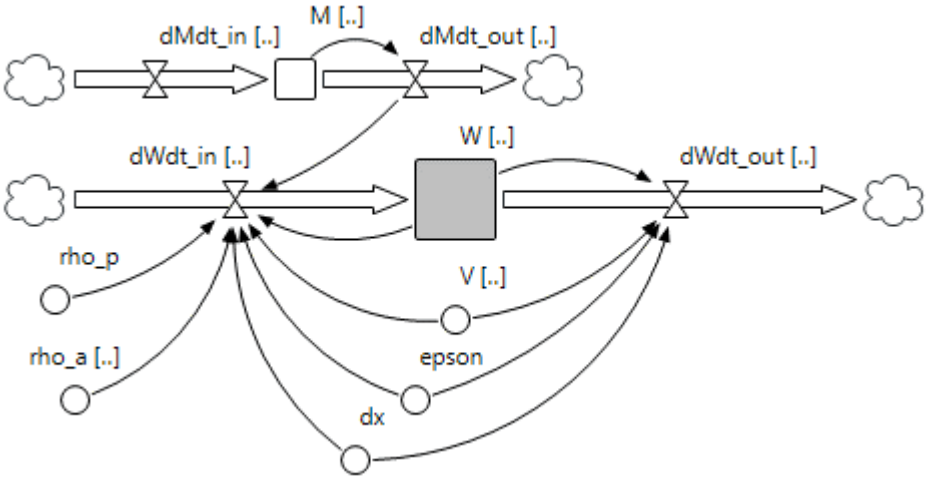

Figure 61. Simplified air humidity ratio flux diagram.

Table 2. Expressions for the fluxes of the stock W.

Index $[i]$ of the layer	**Input flux (dWdt_in)**	**Output flux (dWdt_out)**
0	0 (boundary condition)	0 (boundary condition)
1	$\frac{V[1]}{dx \cdot \varepsilon} W[0] + \frac{\rho_p}{\varepsilon \cdot \rho_a} dMdt\_out[1]$	$\frac{V[1]}{dx \cdot \varepsilon} W[1]$
From 2 to *n*	$\frac{V[i]}{2 \cdot dx \cdot \varepsilon} \cdot 4 \cdot W[i-1] + \frac{\rho_p}{\varepsilon \cdot \rho_a[i]} \cdot dMdt\_out[i]$	$\frac{V[i]}{2 \cdot dx \cdot \varepsilon} (3 \cdot W[i] + W[i-2])$

To obtain the simplified flux diagram of the stock TP – product temperature (theta), equation (3) is used, which corresponds to an energy/enthalpy balance. This expression suggests that the accumulation of energy in the grain (left side of the equality)

depends on the energy used to warm up the product (first term on the right side) and the necessary energy to take out water from it (second term on the right side). Its representation in system dynamics is found in Figure 7. In this case, both the parcels above on the right side of the equation can be considered sources. Thus these are calculated at the flux that enters the stock. The flux that exits is null (dTPdt_out [i]=0).

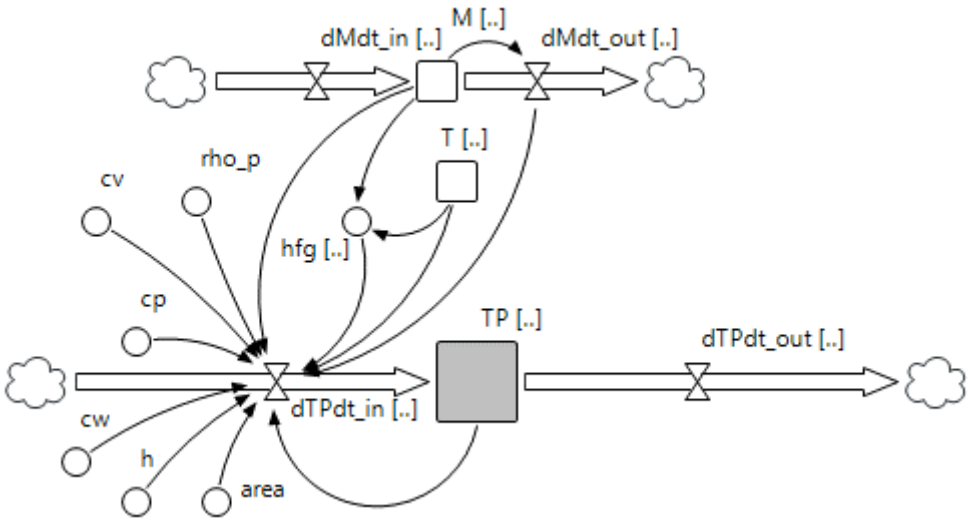

Figure 7. Product temperature simplified flux diagram.

The flux that enters in TP can be calculated using the equation below.

$$dTPdt_{in[i]} = \frac{h \cdot area(T[i]-TP[i])}{\rho_p \cdot C_p} - \frac{\{h_{fg}+C_v \cdot (T[i]-TP[i])\}}{C_p} \cdot dMdt\_out[i] \quad (14)$$

After this demonstration of how are obtained the simplified flux diagrams of the four stocks that make up the deep layer drying model (from Figure 4 to Figure 7), it is possible to perceive that these are dependent among themselves, once the variation rate of each stock (partial derivative) can be expressed as a function of itself, of the other stocks and/or their variation rate, as explicated in the set of equations:

$$\begin{cases} \frac{\partial T}{\partial t} = f(T, W, \theta) \\ \frac{\partial M}{\partial t} = f(M, T) \\ \frac{\partial W}{\partial t} = f(W, \frac{\partial M}{\partial t}) \\ \frac{\partial \theta}{\partial t} = f(\theta, T, M, \frac{\partial M}{\partial t}) \end{cases} \quad (15)$$

Translating to the system dynamics symbology, we have the representation of Figure 8.

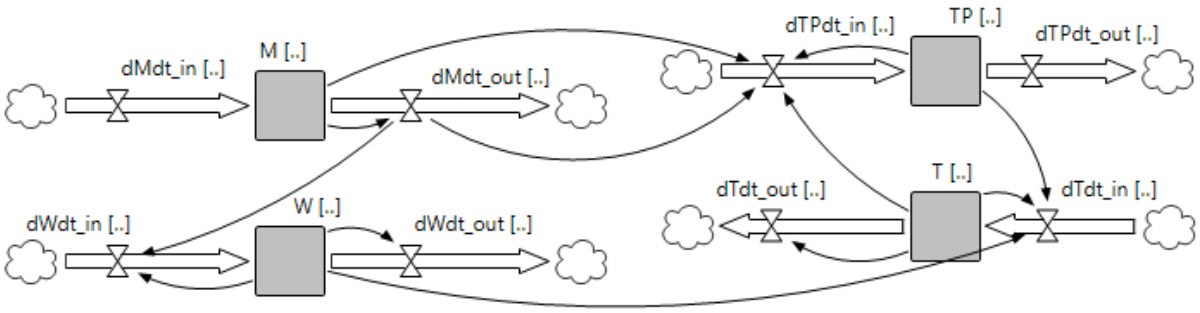

Figure 2. Causal relations between the fluxes and stocks of the drying model.

Suppose we add to this flux diagram the other variables that are on the simplified diagrams. In that case, we obtain the complete flux diagram of the deep layer grain drying model, as presented in Figure 9.

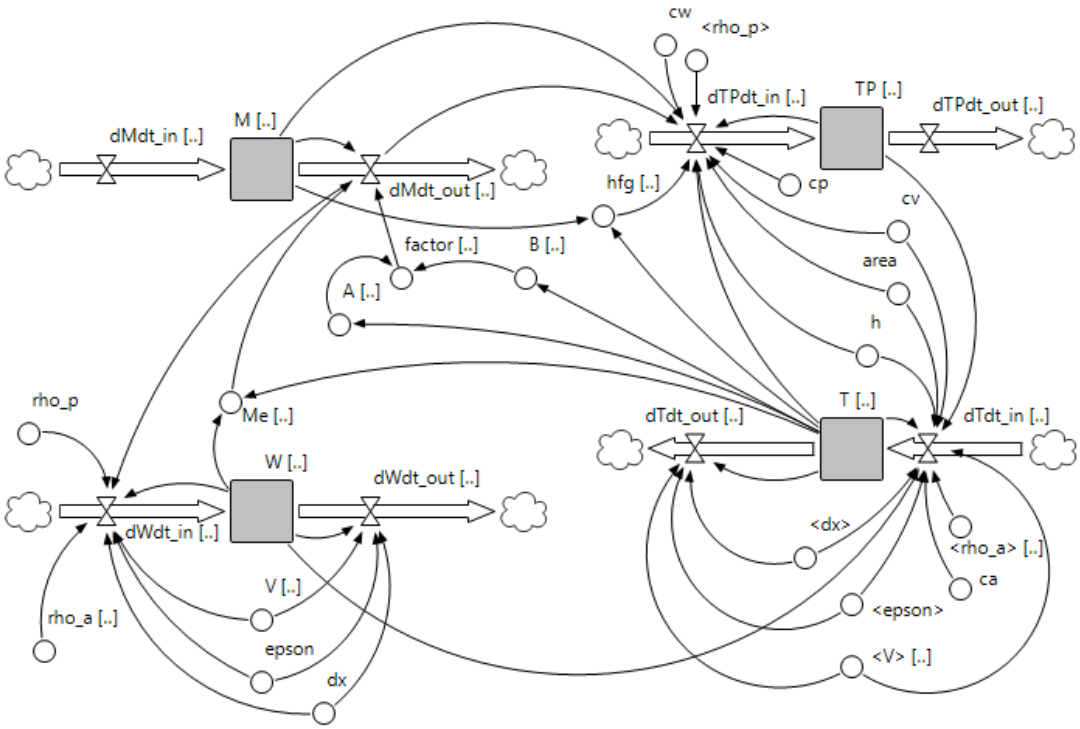

Figure 9. Complete flux diagram of the deep layer grain drying model.

On this complete diagram are all the variables and input data related to the stationary deep layer grain drying process, allowing the simulation of various scenarios and the execution of tests to sensitivity analysis of specific parameters of the process. This diagram represents the fundamental model used to obtain the results of the present work.

It is important to observe that in all the simulations, the number of grain layer subdivisions and the time step must be such that they satisfy the admensional Courant convection condition number [4]:

$$courant = u \cdot \frac{\Delta t}{\Delta x} = \frac{V}{\varepsilon} \cdot \frac{\Delta t}{\Delta x} \leq 1 \qquad (16)$$

To compute the relative humidity, a specific function in this Anylogic model was implemented that uses the psychrometric expression of equation (8) and limits the maximum value of relative humidity to 1.00. In other words, in case the calculated value to be greater, it is substituted by 1.00.

3 RESULTS

3.1 Tests for the validation of the models

To validate the obtained values, the relative error was calculated using the equation:

$$E_R = \frac{|R - S|}{R} \qquad (17)$$

In the case of thermal diffusion, R is found according to the exact analytical solution and S is determined by the proposed model, that is, the system dynamics approach.

The proposed model presents reasonable accuracy when the relative error in each point is less than 1%.

3.2 Pure convection model

For the validation of the pure convection model [equation(6)], the input data of Table 3 were used.

Table 3. Input data for the pure convection example.

Item	Symbol	Value	Unit
Tube length	L	0,6	m
Convection speed	u	0,08	$m \cdot s^{-1}$
Number of simulation segments	N	400	Dimensionless

Due to the problem characteristics, the initial temperature distribution moves to the right with the convection speed, allowing that the exact solution may be easily obtained at any point at any instant.

The simulation results for time 1 s and 9 s are found in Figures

16 and 17, respectively. In these graphics, just 20% of the points used in the calculations are plotted to facilitate the visualization.

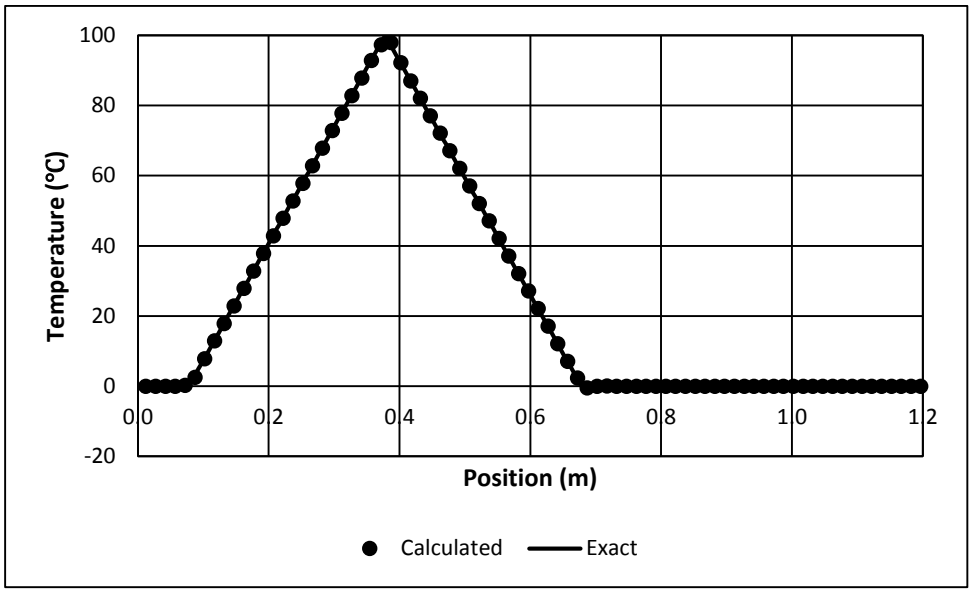

Figure 93. Temperature X position, on-time t=1 s.

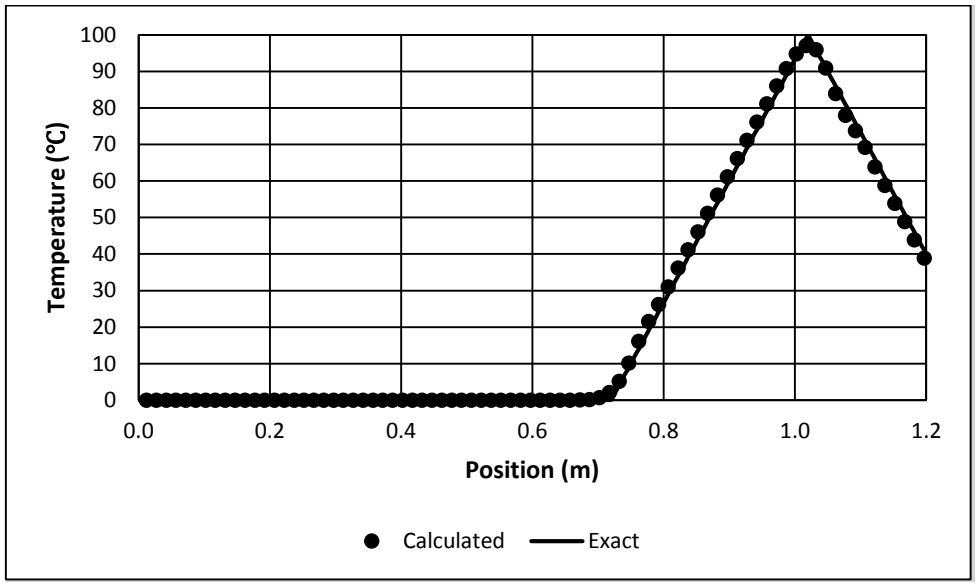

Figure 40. Temperature X position, on-time t=9 s.

To validate the obtained values, the absolute error was calculated, using the exact solution as reference:

$$E_A = |R - S| \quad (18)$$

where R is real, and S is simulated results.

For the time 1 s, the maximum absolute error found was 1.5546℃, and the absolute error mean value 0.1068℃.

For the time 9 s, the maximum absolute error found was 2.9821℃, and the absolute error mean value 0.7962℃.

These results attest to the confirmability of the proposed model.

3.3 One-dimensional deep layer drying model

The physical properties necessary to simulate the corn drying process were extracted from [27]

Figures 11 to 14 present the simulated values (markers) and reference values (lines) of moisture content of the product, humidity ratio, air temperature and product temperature, respectively, all of them in the function of the grain layer depth after 5, 10, 15, and 20 h of drying. The reference curves correspond to numerical data of [28].

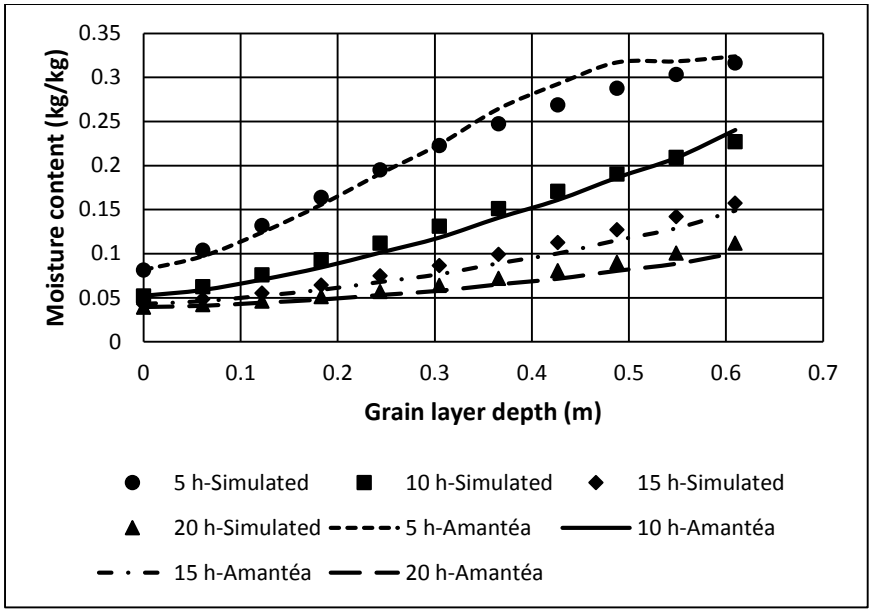

Figure 51. Moisture content of the product X grain layer depth.

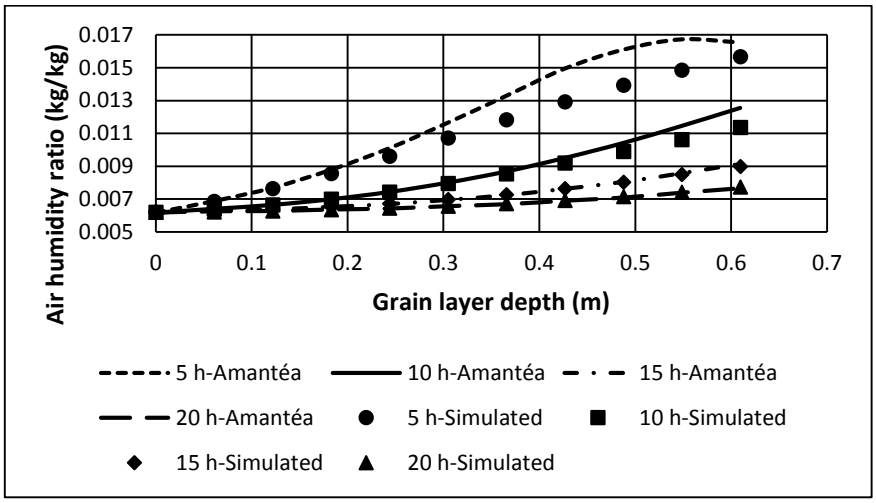

Figure 126. Humidity ratio X grain layer depth.

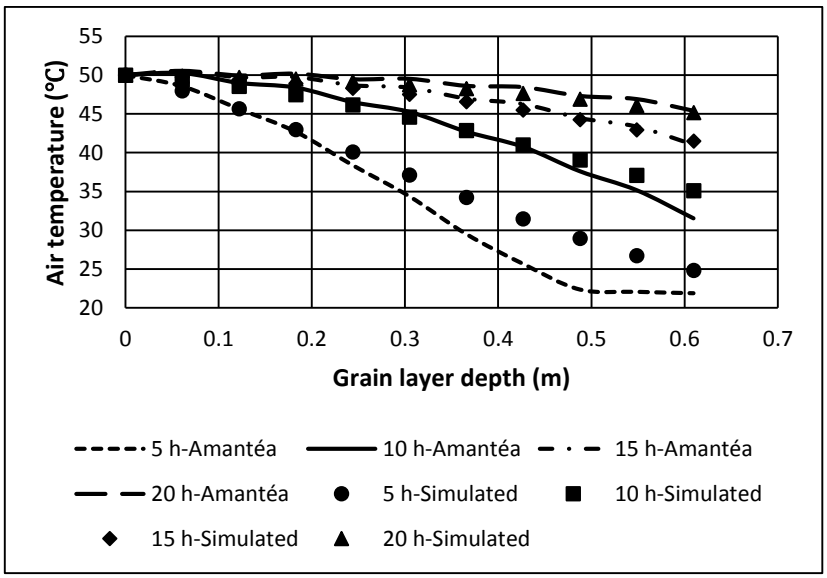

Figure 7. Air temperature X grain layer depth.

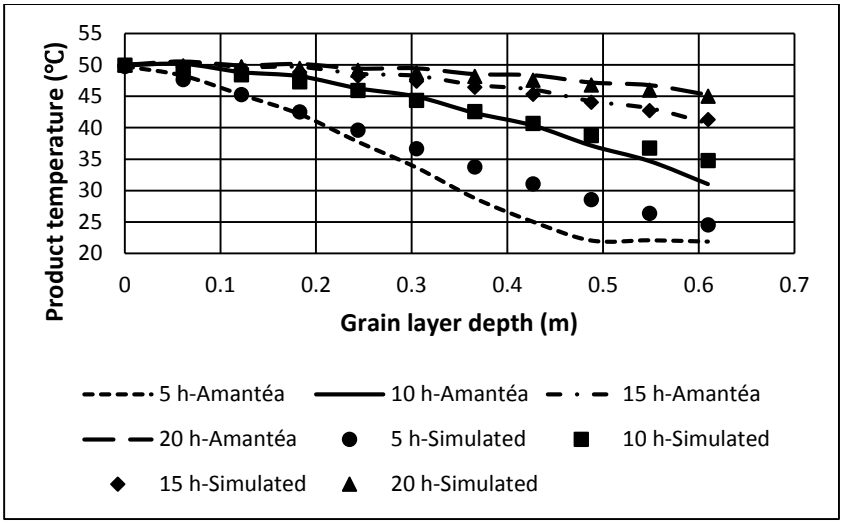

Figure 14. Product temperature X grain layer depth.

To validate the values found in the simulation, using equation (18), the relative error was calculated for each point of these graphics, and the errors arithmetic mean. These calculations were performed by equation, reaching a mean error of around 7% for the moisture content simulation, 2.5% for humidity ratio, and 3.8% for grain and air temperatures.

The behaviors of the main variables are noticeable by the analysis of the graphics. As the drying process advances (greater simulation time), the air and product temperatures increase, tending to stabilize (achieve steady-state) on the baseline of the air temperature on the dryer input. Both remain in equilibrium during all the process. Contrary, as the drying advances, the moisture content of the product decreases.

The humidity ratio presents an elevated growth at the beginning of the simulation and continues until air saturation occurs inside the dryer. It then decreases throughout the rest of the simulation.

The statements above describe the dryer operation: the heated air enters and increases the air and grain temperature. The product cedes water into the air as a consequence. This water saturates the air and is posteriorly removed by its constant flux.

4 CONCLUSIONS

This work developed a one-dimensional model for the simulation of the deep layer grain drying in a fixed bed using the system dynamics. The mass and energy conservation equations and thin layer were discretized and solved for the corn drying case.

By comparing the data generated by the simulations with those of reference obtained by other simulation techniques, we verified that the proposed methodology provides reliable results. The mean of the relative error of the values of each layer of product moisture content, air humidity ratio, air temperature, and product temperature were 7.06%, 2.5%, 3.82%, and 3.89%, respectively. Thus, we can conclude that it is possible to use the present tool to compare varied conditions and different drying scenarios.

It was attested that the differential feature of the system dynamics methodology facilitates the detailed understanding of the physical processes. It is also a technique that does not demand from the user complex knowledge of programming languages and calculus, which is the case of other numerical methods used to solve this problem.

From the data of the simulations, it was verified that it is possible to accelerate the drying procedure by increasing the input air temperature or speed. However, both alterations negatively impact energetic system efficiency. The developers of dryers and producers must be aware of the perturbations of these variables on the product quality, once this fact was not in the scope of this research.

As future works suggestions, we can cite the coupling of spatial models of grain quality analysis and populational growth of plagues to the main diagram here proposed and the implementation of optimization techniques. We also plan to evolve the suggested causal diagram to a flux diagram, with all the necessary computation expressions

REFERENCES

[1] Ribeiro, G. 2015. "Simulação de secagem de soja (Glycine max L. Merril) variedade monsoy 9144RR, em camada estacionária", Master Dissertation, Federal University of Viçosa, Brazil.

[2] Jangam, S. V.; Law, C. L.; Mujumdar, A. S. 2010, "Drying of foods, vegetables and fruits" Singapore.

[3] Santos, G.T, Fortes, M,, Amantéa, R.P,Ferreira, W. R.,Martins, J. H. 2018. "Irreversible thermodynamics analysis of ellipsoidal wheat kernel drying, aiming at the evaluation of phenomenological properties", Drying Technology, 36:9, 1117-1127.

[4] Hoffman, J. D. 1992. "Numerical methods for engineers and scientists**".** New York: McGraw-Hill, v. 34.

[5] Amantéa, R. P., De Carvalho, R. Barbosa, L.O. 2021, "Evaluation of a radial basis function node refinement algorithm applied to bioheat transfer modeling" AIMS-Bioengineering, Volume 8, Issue 1: 36-51.

[6] Hussain, M. M.; Dincer, I.2003. "Two-dimensional heat and moisture transfer analysis of a cylindrical moist object subjected to drying: A finite-difference approach.", International Journal of Heat and Mass Transfer, v. 46, n. 21, p. 4033–4039.

[7] França, A. S.; Fortes, M.; Haghighi, K. 1994. "Numerical simulation of intermittent and continuous deep-bed drying of biological materials." Drying Technology, v. 12, p. 1537-1560.

[8] Song, C. S., Nam, J.H, , Kim, C.-J., Ro, S. T. 2002. "A finite volume analysis of vacuum freeze drying processes of skim milk solution in trays and vials." Drying Technology, v. 20, n.2, p. 283–305.

[9] Liu, Z., Wu, Z., Wang, X. 2015. "Numerical simulation and experimental study of deep bed corn drying based on water potential" Mathematical Problems in Engineering, v.4, 1-13.

[10] Srivastava, V. K.; John, J. 2022. "Deep bed grain drying modeling." Energy conversion and management, v. 43, n. 13, p. 1689-1708,

[11] Dalpasquale, V. A, Esperandio, D., Silva, L.H.M, Kolling, E. 2008. "Fixed-bed drying simulation of agricultural products using a new backward finite difference scheme". Applied mathematics and computation, v. 200, n. 2, p. 590-595.

[12] Sitompul, J P.; Istadi; W., Nyoman.I. 2001. "Modeling and simulation of deep-bed grain dryers". Drying Technology, v. 19, n. 2, p. 269-280,

[13] Borges, P. A. P. 2002. "Modelagem dos processos envolvidos nos sistemas de secagem e de armazenamento de grãos.**"**. PhD Thesis Federal University of Rio Grande do Sul, Porto Alegre, Brazil.

[14] Franca,A.S., Fortes,M., Haghighl,K. 1994 "Numerical simulation of intermittent and continuous deep-bed drying of biological materials", Drying Technology, 12:7, 1537-1360.

[15] GARCÍA, J. M. 2006. "Theory and practical exercises of system dynamics". MIT Sloan School of Management.

[16] Kirkwood, C W. 1998. "System dynamics methods: a quick introduction". College of Business Arizona State University USA.

[17] Prado, A. A. 2013. "Contribuição da abordagem System Dynamics na compreensão da competitividade de clusters de negócios". Revista Ibero Americana de Estratégia, v. 12, n. 4.

[18] Franco, R. A. C; YOSHIZAKI, Yoshida, H. T. ; VIEIRA, J. G. V. 2016. "A system dynamics approach to logistics outsourcing policies and decisions". Production, v. 26, n. 2, p. 285-302.

[19] Wang, Y.; Li, Y; Guo, P.. 2015. "Modelling Construction Project Management Based on System Dynamics". **Metallurgical & Mining Industry**, n. 9.

[20] Martins, J. H., Camanho, ,A.S., Oliveira, M.M.,Gaspar, M.B.2015. "A system dynamics model to support the management of artisanal dredge fisheries in the south coast of Portugal". International Transactions in Operational Research, v. 22, n. 4, p. 611-634.

[21] Simonetto, E. O., Putnik, G. , Rodrigues, G. O., Alves, C., Castro, H. 2016. "Um modelo de dinâmica de sistemas para avaliação do reaproveitamento de resíduos eletrônicos na remanufatura de computadores em uma instituição de ensino superior". Exacta, v. 14, n. 3.

[22] Xie, T., ,Benjamin, W. B. D. , Liu, A. X. ,Gray, G. C. 2017. "A system dynamics approach to understanding the One Health concept." PloS one, v. 12, n. 9, p. e0184430.

[23] Walters, J. P., Archer, D. W, Sassenrath, G. F., Hendrickson, J. R., Hanson, J. D., Halloran, J. M., Vadas, P. , Alarcon, V. J. 2016. "Exploring agricultural production systems and their fundamental components with system dynamics modelling." **Ecological Modelling**, v. 333, p. 51–65, 2016.

[24] Gonçalves, J. C. de S. I, Marcius F. 2013. "Mathematical model for the simulation of water quality in rivers using the Vensim PLE software". Journal of Urban and Environmental Engineering, v. 7, n. 1,.

[25] Brooker, D. B.; Bakker-Arkema, F. W.; Hall, C. W. 1992 "Drying and storage of grains and oilseeds." Springer Science & Business Media.

[26] Fortes, M; Ferreira, W. R.. 2004. "Second law analysis of drying; Modeling and simulation of fluidized bed grain drying." In: Drying 2004, Proceedings of the 14th International Drying Symposium IDS 2004**.** 2004. p. 301-308.

[27] Brooker, D. B.; Bakker-Arkema, F. W.; Hall, C. W.1974. "Drying Cereal Grains.**"** The AVI Pub. Co. Inc. West Port, Connecticut, USA.

[28] Amantea, R. P. 2008. "Metodologia numérica para análise de secagem de grãos em leito fixo pela primeira e segunda Lei da Termodinâmica.". Master Dissertation , Federal University of Viçosa, Brazil.

LIST OF SYMBOLS

a	Grain kernel area per unit bed volume, $m^2 \cdot m^{-3}$
A	Empirical thin layer drying equation parameter
B	Empirical thin layer drying equation parameter
c_a	Specific heat (drying air), $J \cdot kg^{-1} \cdot K^{-1}$
c_p	Specific heat (product), $J \cdot kg^{-1} \cdot K^{-1}$
c_v	Specific heat (water vapor), $J \cdot kg^{-1} \cdot K^{-1}$
c_w	Specific heat (water), $J \cdot kg^{-1} \cdot K^{-1}$
dx	Bed height, m

dy Spatial coordinate , m

EA Absolute error

ER Relative error

h' Convective heat transfer, $W \cdot m^{-2} \cdot K^{-1}$

h_{fg} latent heat of vaporization for corn, $J \cdot kg^{-1}$

L Length, m

$\dot{m}_a$ Dry air mass flow rate, $kg \cdot s$

m_s Dry mass, *kg*

M Moisture content of grain (Dry basis) $kg \cdot kg^{-1}$

M_0 Initial moisture content (Dry basis), $kg \cdot kg^{-1}$

M_e Equilibrium moisture content (Dry basis), $kg \cdot kg^{-1}$

M_t Average moisture content (dry basis), $kg \cdot kg^{-1}$

P Pressure, Pa

pv Vapor pressure, Pa

RH Relative humidity

t Time, s

T Dry air temperature, $^{\circ}C$

T_0 Initial product temperature, $^{\circ}C$

T_s Drying air temperature, $^{\circ}C$

u Convective parameter, $m \cdot s^{-1}$

V Drying air velocity, $m \cdot s^{-1}$

W Humidity ratio $kg \cdot kg^{-1}$

x Spatial coordinate (bed), m

y Spatial coordinate, m

α Diffusion coefficient, $m^2 \cdot s^{-1}$

Δt Time step, s

ε Porosity, *decimal*

η First law efficiency, *decimal*

θ Product temperature, $^{\circ}C$

ρ_a Dry air density, $kg \cdot m^{-3}$

ρ_p Product density, $kg \cdot m^{-3}$